

The role of ventral striatal cAMP signaling in stress-induced behaviors

Florian Plattner¹, Kanehiro Hayashi^{1,12}, Adan Hernández¹, David R Benavides^{1,12}, Tara C Tassin¹, Chunfeng Tan¹, Jonathan Day², Maggy W Fina³, Eunice Y Yuen⁴, Zhen Yan⁴, Matthew S Goldberg^{1,5}, Angus C Nairn^{6,7}, Paul Greengard⁷, Eric J Nestler⁸, Ronald Taussig³, Akinori Nishi⁹, Miles D Houslay¹⁰ & James A Bibb^{1,5,11}

The cAMP and cAMP-dependent protein kinase A (PKA) signaling cascade is a ubiquitous pathway acting downstream of multiple neuromodulators. We found that the phosphorylation of phosphodiesterase-4 (PDE4) by cyclin-dependent protein kinase 5 (Cdk5) facilitated cAMP degradation and homeostasis of cAMP/PKA signaling. In mice, loss of Cdk5 throughout the forebrain elevated cAMP levels and increased PKA activity in striatal neurons, and altered behavioral responses to acute or chronic stressors. Ventral striatum- or D1 dopamine receptor-specific conditional knockout of Cdk5, or ventral striatum infusion of a small interfering peptide that selectively targeted the regulation of PDE4 by Cdk5, produced analogous effects on stress-induced behavioral responses. Together, our results demonstrate that altering cAMP signaling in medium spiny neurons of the ventral striatum can effectively modulate stress-induced behavioral states. We propose that targeting the Cdk5 regulation of PDE4 could be a new therapeutic approach for clinical conditions associated with stress, such as depression.

The cAMP/PKA signaling pathway acts as an important integrator of actions from various neuromodulators, critically regulating CNS functions, including neuronal survival, axonal regeneration and cognition¹. The activity of the cAMP/PKA cascade is tightly controlled to maintain the specificity and integrity of the intracellular signal propagation. Neuromodulators, such as dopamine, stimulate G protein-coupled receptors that in turn trigger cAMP synthesis by adenylyl cyclases¹. Hydrolysis of cAMP by cyclic nucleotide phosphodiesterases (PDEs) counteracts adenylyl cyclase function, thereby reducing cAMP levels¹. The enzymatic activity of PDEs can also be regulated by multiple converging intracellular signaling pathways². For example, cAMP hydrolysis by PDE4 is controlled via phosphorylation by the cAMP downstream target PKA, as part of a negative feedback loop^{3,4}. Another protein kinase linked with the regulation of cAMP/PKA signaling is Cdk5, for which a reciprocal regulatory relationship with PKA has been observed in medium spiny neurons of the striatum⁵. However, the underlying molecular processes of this interaction are not yet completely understood.

Cdk5 is a proline-directed serine/threonine kinase that requires association with its cofactors, p35 and p39, for activation⁶. Cdk5 is involved in various CNS functions, including neuronal migration, neurotransmission and memory formation^{6–8}. Dysfunction of Cdk5

has been associated with several neurological and neuropsychiatric disorders^{9–11}. Increases in expression of Cdk5 and its activator p35 have been observed in response to stress in various brain areas of the limbic system, including the basolateral amygdala and septohippocampal system^{12–14}. Consistent with these results, reduced sucrose preference and locomotor activity in response to chronic mild stress were mitigated by infusion of a Cdk5 inhibitor into the hippocampal subfield dentate gyrus¹⁵. In contrast, loss of Cdk5 in dopamine neurons of the ventral tegmental area has been suggested to decrease dopamine-release in ventral striatum, reduce motor activity in response to acute stress, prolong novel environment-related feeding delay and attenuate sucrose preference¹⁶.

The limbic system controls emotional behavior and motivational drives and is important for the neurobiological response to stress. A variety of behavioral stress procedures have been linked to dopamine release in the striatum^{17,18}. Recent studies have implicated dopaminergic inputs into medium spiny neurons of the ventral striatum with stress-induced behaviors^{19,20}. Despite some progress, the pathophysiological basis of major depressive disorder (MDD), which may be triggered or exacerbated by severe or chronic stress, remains unclear. We identified a previously unknown regulatory mechanism of cAMP/PKA signaling present in the ventral striatum that

¹Department of Psychiatry, The University of Texas Southwestern Medical Center, Dallas, Texas, USA. ²Division of Neuroscience and Molecular Pharmacology, Institute of Biomedical and Life Sciences, University of Glasgow, Glasgow, UK. ³Department of Pharmacology, The University of Texas Southwestern Medical Center, Dallas, Texas, USA. ⁴Department of Physiology and Biophysics, State University of New York at Buffalo, Buffalo, New York, USA. ⁵Department of Neurology and Neurotherapeutics, The University of Texas Southwestern Medical Center, Dallas, Texas, USA. ⁶Department of Psychiatry, Yale University School of Medicine, New Haven, Connecticut, USA. ⁷Laboratory of Molecular and Cellular Neuroscience, The Rockefeller University, New York, New York, USA. ⁸Fishberg Department of Neuroscience and Friedman Brain Institute, Icahn School of Medicine at Mount Sinai, New York, New York, USA. ⁹Department of Pharmacology, Kurume University School of Medicine, Fukuoka, Japan. ¹⁰Institute of Pharmaceutical Science, King's College London, London, UK. ¹¹Harold C. Simmons Comprehensive Cancer Center, The University of Texas Southwestern Medical Center, Dallas, Texas, USA. ¹²Present addresses: Department of Anatomy, Keio University School of Medicine, Tokyo, Japan (K.H.), and Department of Neurology, The Johns Hopkins University School of Medicine, Baltimore, Maryland, USA (D.R.B.). Correspondence should be addressed to J.A.B. (james.bibb@utsouthwestern.edu).

Received 27 April; accepted 19 June; published online 20 July 2015; doi:10.1038/nn.4066

involves the phosphorylation of PDE4 by Cdk5 and showed that it can modulate behavioral responses to acute and chronic stress.

RESULTS

Cdk5 regulates cAMP signaling via phosphorylation of PDE4

Various intracellular signaling pathways converge onto PDE4, thereby regulating cAMP/PKA signaling². As a reciprocal regulatory relationship exists between PKA and Cdk5 activity⁵, we hypothesized that PDE4 might serve as an important mediator of the interaction between Cdk5 and PKA. To address this idea, we first assessed whether Cdk5 might regulate PDE4 via protein phosphorylation. Indeed, PDE4 was efficiently phosphorylated by Cdk5 at a serine residue (Ser145 in the long PDE4B1 isoform) 12 amino acids C-terminal to the well-characterized PKA site (Ser133 in PDE4B1), both of which were located in the regulatory upstream conserved region 1 (UCR1) (Fig. 1a,b and Supplementary Fig. 1a,b) and were conserved in all long PDE4 forms (Fig. 1b). Members of the PDE4 subfamilies were expressed throughout the adult brain, with PDE4B isoforms being particularly prominent in striatum, including the nucleus accumbens (NAc, part of the ventral striatum), where Cdk5 was also abundant (Supplementary Fig. 1c). PDE4 phosphorylation levels in pharmacologically treated brain slices were assessed with phospho-specific antibodies to the Cdk5 and PKA sites (Supplementary Fig. 1d–f). Treatment of striatal slices with the adenyl cyclase activator forskolin consistently increased PDE4 phosphorylation by PKA (Supplementary Fig. 1e), whereas Cdk5 inhibition by indolinone A decreased PDE4 phosphorylation selectively at the Cdk5 site (Supplementary Fig. 1f).

Next we evaluated Cdk5-dependent regulation of PDE4 activity and cAMP levels. Application of the Cdk5 inhibitor roscovitine to mouse striatal lysate decreased PDE activity, whereas recombinant active Cdk5 increased PDE activity (Fig. 1c). Accordingly, roscovitine elevated cAMP to comparable levels as the D1 receptor agonist SKF81297 in striatal slices (Fig. 1d), suggesting that Cdk5 potentiates PDE4 activity and thereby downregulates cAMP levels. Moreover, the Cdk5

inhibitor indolinone A slowed cAMP degradation following stimulation of G protein-coupled receptors by isoproterenol, as assessed in an in-cell bioluminescence resonance energy transfer (BRET) sensor assay (Fig. 1e). Levels of cGMP were not affected by treatment of striatal slices with indolinone A (Supplementary Fig. 1g).

As PKA phosphorylation activates PDE4 long isoforms^{3,4}, and the two sites are located in close proximity in the UCR1, we investigated their potential functional interactions and found that Cdk5 inhibition attenuated PDE4 phosphorylation at the PKA site (Fig. 1f). Furthermore, mutating the Cdk5 site from serine to alanine attenuated forskolin-induced phosphorylation of PDE4 by PKA (Fig. 1g). In other experiments, mimicking constitutive phosphorylation at the Cdk5 site (Ser145Asp) led to a significant, but modest (1.2-fold, $P = 0.008$), increase in PDE4 activity, whereas phosphomimetic mutation of the PKA site (Ser133Asp) increased PDE4 activity 1.9-fold (Fig. 1h). Phosphomimetic replacement at both sites (Ser133Asp/Ser145Asp) increased PDE4 activity 2.5-fold, indicating a synergistic interaction in which UCR1 phosphorylation by Cdk5 primes subsequent phosphorylation by PKA, and dual phosphorylation at these sites potentiates PDE4 activation. Given that Cdk5 can regulate cAMP levels via PDE4, we assessed the effect of Cdk5 inhibition on cAMP signaling by evaluating the phosphorylation state of several PKA substrates in striatal slices. Roscovitine induced PKA-dependent phosphorylation of CREB (Ser133) and synapsin (Ser9), and, consistent with previous studies⁵, increased phosphorylation of DARPP-32 (Thr34) and the AMPA receptor subunit GluR1 (Ser845; Supplementary Fig. 2a). Moreover, the phosphorylation of DARPP-32 by PKA and Cdk5 exhibited a dose-dependent reciprocal relationship (Supplementary Fig. 2b).

Cdk5 cKO mice exhibit elevated cAMP signaling and altered stress-induced behavioral responses

To further explore the role of Cdk5 in cAMP/PKA signaling *in vivo*, we analyzed an inducible conditional Cdk5 knockout (Cdk5 cKO) mouse model. Neuronal-specific knockdown of Cdk5 throughout

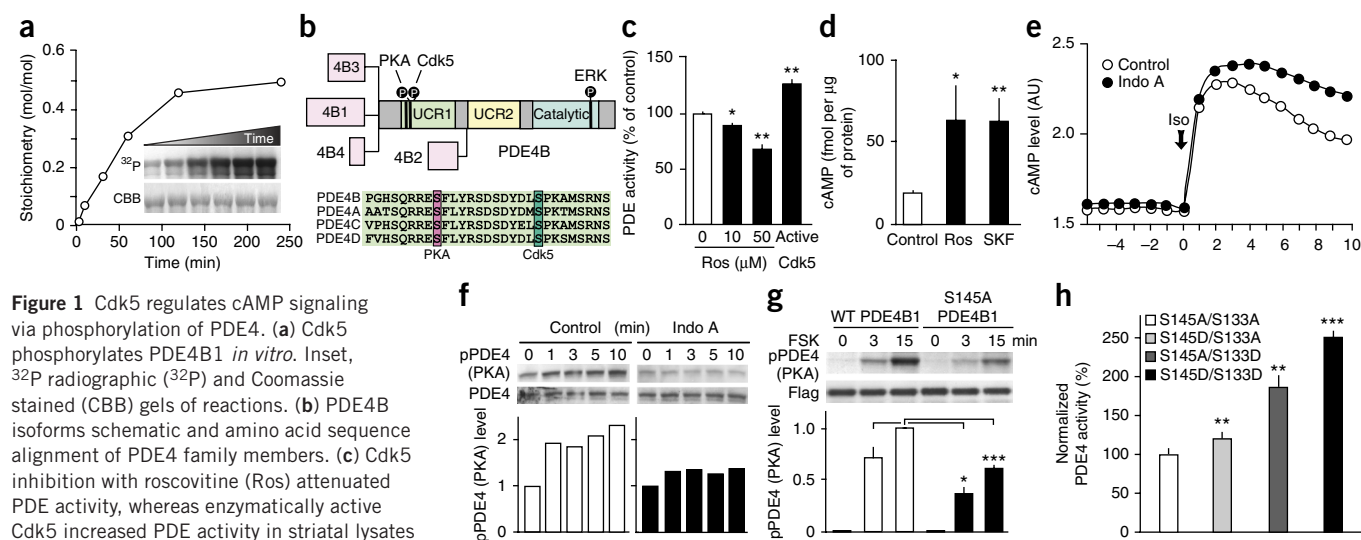


Figure 1 Cdk5 regulates cAMP signaling via phosphorylation of PDE4. (a) Cdk5 phosphorylates PDE4B1 *in vitro*. Inset, ³²P radiographic (³²P) and Coomassie stained (CBB) gels of reactions. (b) PDE4B isoforms schematic and amino acid sequence alignment of PDE4 family members. (c) Cdk5 inhibition with roscovitine (Ros) attenuated PDE activity, whereas enzymatically active Cdk5 increased PDE activity in striatal lysates ($n = 4$ slices; Ros 10 μ M, $P = 0.011$; Ros 50 μ M, $P = 0.0037$; Cdk5/p25, $P = 0.006$). (d) Cdk5 inhibition with Ros and D1 receptor activation using SKF81297 (SKF) increased cAMP to similar levels in striatal slices (control and Ros, $n = 3$ slices; SKF, $n = 4$ slices; Ros, $P = 0.0216$; SKF, $P = 0.0030$). (e) Cdk5 inhibition with indolinone A (Indo A, 10 μ M) reduced cAMP hydrolysis after stimulation with isoproterenol (Iso, 30 nM). (f) PKA-dependent activation of PDE4 was attenuated by Indo A. (g) Mutation of the Cdk5 site Ser145 to Ala in PDE4B1 (S145A PDE4B1) reduced PKA-mediated PDE4 phosphorylation after forskolin (FSK, 10 μ M) treatment in PC12 cells ($n = 8$ reactions; WT versus S145A at 3 min, $P = 0.0241$; WT versus S145A at 15 min, $P < 0.0001$). (h) Mutational analysis of the relative contributions of the Cdk5- and PKA-dependent PDE4 phosphorylation sites to PDE activity ($n = 4$ reactions; S145D/S133A versus S145A/S133A, $P = 0.0082$; S145A/S133D versus S145A/S133A, $P = 0.0019$; S145D/S133D versus S145A/S133A, $P < 0.0001$). Whole immunoblot images are presented in Supplementary Figure 13. All data shown are means \pm s.e.m. * $P < 0.05$, ** $P < 0.01$, *** $P < 0.001$.

forebrain was achieved by crossing homozygous floxed *Cdk5* mice with animals bearing a tamoxifen-inducible Cre-ERT recombinase transgene under the control of the prion protein promoter²¹. In this mouse line, Cre-ERT recombinase expression is low or absent in areas of the midbrain, such as ventral tegmental area and substantia nigra²². However, *Cdk5* expression ($P < 0.001$) and activity ($P < 0.01$) was significantly reduced in striatal medium spiny neurons of *Cdk5* cKO mice compared with wild-type (WT) littermate controls (Fig. 2a–c and Supplementary Fig. 3a). Consequently, dorsal and ventral striatal *Cdk5*-dependent PDE4 phosphorylation was decreased (Fig. 2b,c and Supplementary Fig. 3b). In agreement with the observation that *Cdk5* primes PKA-dependent PDE4 phosphorylation, the phosphorylation state at the PKA site was also reduced (Supplementary Fig. 3c). The reduction in PDE4 phosphorylation at the *Cdk5* and PKA sites coincided with elevated cAMP levels (Fig. 2d). Striatal levels of cGMP, as well as monoamines such as dopamine (DA) and serotonin (5-HT), were unchanged in *Cdk5* cKO mice (Supplementary Fig. 3d and Supplementary Table 1). The elevation in cAMP levels correlated with increased PKA-dependent phosphorylation of DARPP-32 and GluR1 (Fig. 2e). Accordingly, activation of G_s -coupled A2A adenosine receptors did not cause PDE4 phosphorylation by PKA (Fig. 2f). To further test whether PKA function is altered in *Cdk5* cKO mice, we performed whole-cell patch-clamp recordings and assessed the effect of PKA inhibition on NMDA receptor currents

in striatal neurons. PKA inhibition with the cell-permeable inhibitor PKI₁₄₋₂₂ reduced NMDA receptor current in striatal neurons from WT mice (Supplementary Fig. 4a–c). This effect was attenuated in neurons from *Cdk5* cKO mice, likely as a result of the increase in PKA activity. Notably, basal NMDA receptor current density was decreased in *Cdk5* cKO mice (Supplementary Fig. 4d–f), which correlated with decreased spine density, but no change in spine type proportion (Supplementary Fig. 5a,b). Together, these results indicate that PDE4 activation is impaired in *Cdk5* cKO mice, consistent with our *in vitro* analyses.

Given that *Cdk5* loss resulted in potentiated striatal cAMP/PKA signaling, we assessed the behavioral effects of *Cdk5* cKO in acute and chronic stress procedures. *Cdk5* cKO mice showed markedly reduced immobility and increased latency to initiation of floating in the Porsolt forced-swim test (FST) compared with WT (Fig. 2g). Consistent with this effect, *Cdk5* cKO mice struggled longer in the tail-suspension test (TST; Fig. 2h). Moreover, *Cdk5* cKO mice exhibited increased social interaction after chronic social defeat stress (SD) (Fig. 2i). *Cdk5* cKO mice spent more time in the interaction zone and less in the corners than controls (Supplementary Fig. 5c). In the sucrose preference test (SPT), a test of anhedonia that does not rely on locomotor activity²³, *Cdk5* cKO mice favored sucrose over water significantly more (Fig. 2j). Furthermore, chronic unpredictable stress (CUS) significantly reduced sucrose preference in WT mice ($P < 0.05$), but had no effect

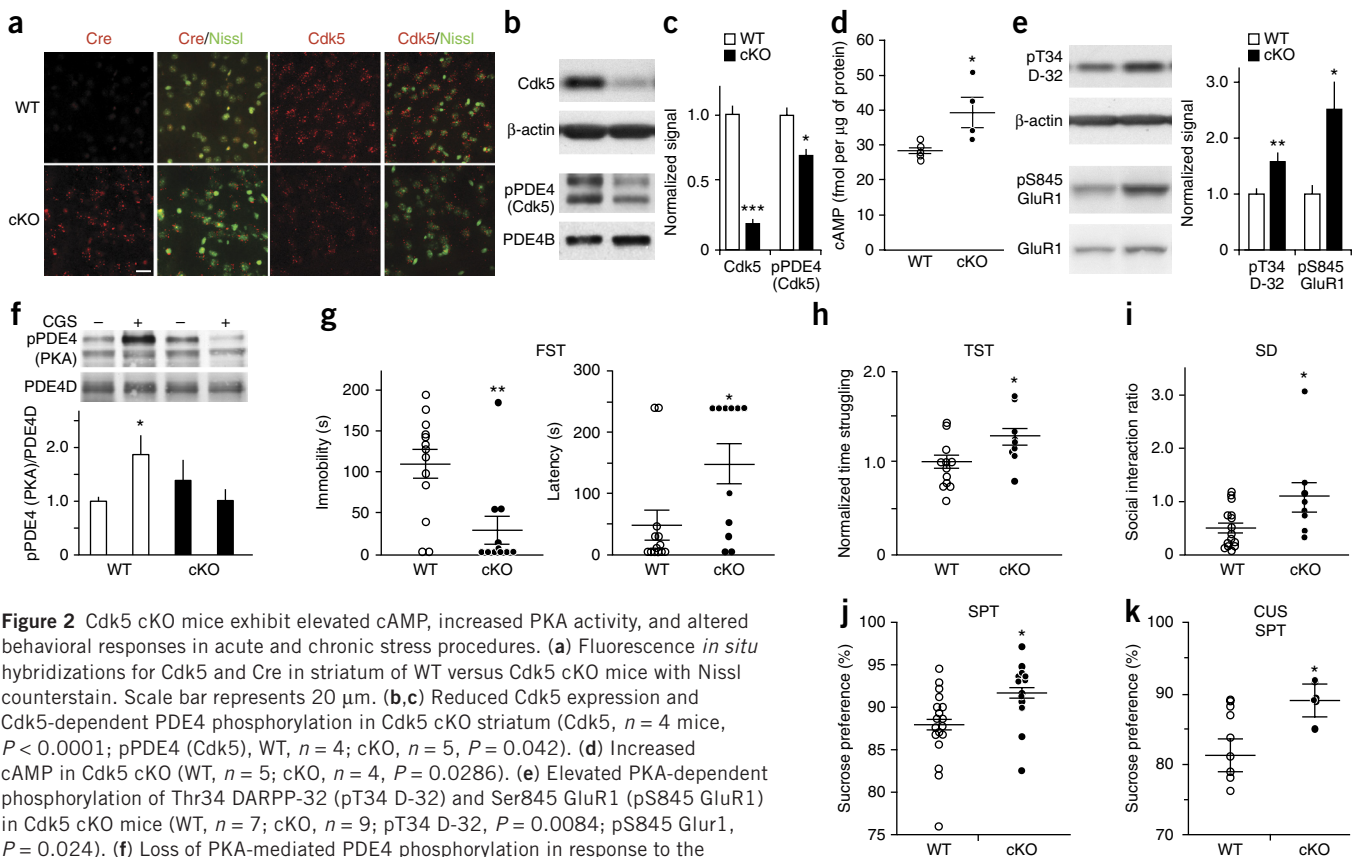


Figure 2 *Cdk5* cKO mice exhibit elevated cAMP, increased PKA activity, and altered behavioral responses in acute and chronic stress procedures. (a) Fluorescence *in situ* hybridizations for *Cdk5* and Cre in striatum of WT versus *Cdk5* cKO mice with Nissl counterstain. Scale bar represents 20 μ m. (b,c) Reduced *Cdk5* expression and *Cdk5*-dependent PDE4 phosphorylation in *Cdk5* cKO striatum (*Cdk5*, $n = 4$ mice, $P < 0.0001$; pPDE4 (*Cdk5*), WT, $n = 4$; cKO, $n = 5$, $P = 0.042$). (d) Increased cAMP in *Cdk5* cKO (WT, $n = 5$; cKO, $n = 4$, $P = 0.0286$). (e) Elevated PKA-dependent phosphorylation of Thr34 DARPP-32 (pT34 D-32) and Ser845 GluR1 (pS845 GluR1) in *Cdk5* cKO mice (WT, $n = 7$; cKO, $n = 9$; pT34 D-32, $P = 0.0084$; pS845 GluR1, $P = 0.024$). (f) Loss of PKA-mediated PDE4 phosphorylation in response to the adenosine A2A receptor agonist CGS21680 (CGS, 5 μ M, 2 min) in *Cdk5* cKO striatum ($n = 4$ slices from 2 mice; WT CGS versus cKO CGS, $P = 0.0354$). (g–k) *Cdk5* cKO mice exhibited altered stress-induced behavior in the FST with reduced immobility time and increased latency to initiation of floating (WT, $n = 13$; cKO, $n = 11$; immobility, $P = 0.0035$; latency, $P = 0.0201$); (g), in the TST with increased time struggling (WT, $n = 12$; cKO, $n = 9$, $P = 0.0281$); (h), in SD with elevated social interaction ratio as the *Cdk5* cKO showed reduced avoidance (WT, $n = 15$; cKO, $n = 8$, $P = 0.0309$); (i), and in the SPT, a measure of anhedonia, with increased sucrose preference (WT, $n = 19$; cKO, $n = 13$, $P = 0.0156$); (j), which persisted after exposure to chronic unpredicted stress (WT, $n = 10$; cKO, $n = 6$, $P = 0.0497$); (k). Whole immunoblot images are presented in Supplementary Figure 13. All data shown are means \pm s.e.m. * $P < 0.05$, ** $P < 0.01$, *** $P < 0.001$.

Figure 3 Virus-mediated Cdk5 knockout in ventral striatum reduces PDE4 phosphorylation and alters stress-induced behaviors. **(a)** Immunostaining showing virus-mediated Cdk5 knockout in NAC neurons of homozygous floxed Cdk5 (*loxP/loxP* AAV) mice. **(b,c)** Reduced Cdk5 expression and PDE4 phosphorylation at the Cdk5 and PKA sites in ventral striatum of *loxP/loxP* AAV mice (WT, $n = 4$; *loxP/loxP* AAV, $n = 5$; Cdk5, $P = 0.0037$; pPDE4 (Cdk5), $P = 0.0164$; pPDE4 (PKA), $P = 0.0176$). **(d–h)** Effect of AAV2-Cre-mediated Cdk5 loss in ventral striatum on behavioral responses to acute and chronic stress procedures. The *loxP/loxP* AAV mice showed reduced immobility time in FST (WT, $n = 6$; *loxP/loxP* AAV, $n = 7$; $P = 0.0065$; **d**), increased time struggling in TST (WT, $n = 12$; *loxP/loxP* AAV, $n = 9$; $P = 0.04225$; **e**), increased social interaction ratio in SD (WT, $n = 9$; *loxP/loxP* AAV, $n = 10$; $P = 0.0314$; **f**), and elevated sucrose preference in SPT ($n = 5$ mice, $P = 0.0116$; **g**), as well as in the CUS procedure (WT, $n = 6$; *loxP/loxP* AAV, $n = 5$; $P = 0.0027$; **h**). Whole immunoblot images are presented in **Supplementary Figure 13**. All data shown are means \pm s.e.m. * $P < 0.05$, ** $P < 0.01$, *** $P < 0.001$.

in Cdk5 cKO (**Fig. 2k**). Cdk5 cKO mice exhibited normal anxiety-like and locomotor behavior as well as baseline social interaction (**Supplementary Fig. 5d,e**; also see ref. 21).

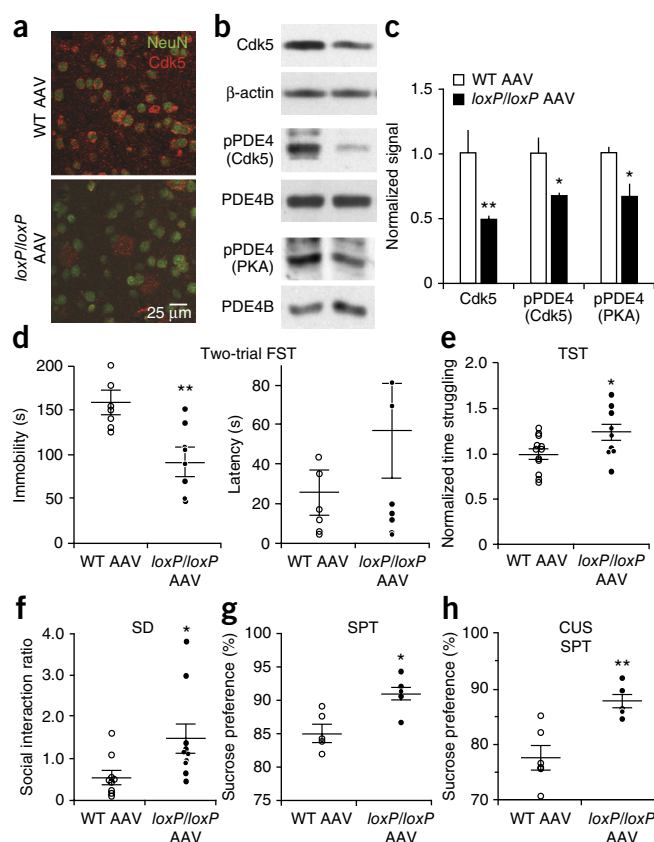
Given that mice with altered PDE4 phosphorylation and cAMP/PKA signaling exhibited altered behavioral response to stress, we next evaluated whether behavioral stressors could also affect PDE4 phosphorylation. PDE4 phosphorylation at the PKA site was increased 1 h after FST, but not at the Cdk5 site (**Supplementary Fig. 6a,b**). In response to SD, PDE4 phosphorylation at both the PKA and Cdk5 sites was increased 1 h after social interaction testing (**Supplementary Fig. 6c,d**). Comparably, exposure to CUS increased PDE4 phosphorylation at the PKA and Cdk5 sites (**Supplementary Fig. 6e,f**). Together, these findings suggest that Cdk5/PKA-dependent PDE4 activation is an important modulator of behavioral responses to stress.

cAMP signaling in the ventral striatum contributes to behavioral responses to stress

Recent studies have implicated dopaminergic inputs into medium spiny neurons of the ventral striatum in behavioral responses to stress^{19,20,24}. To assess whether medium spiny neurons in the ventral striatum specifically employ Cdk5-dependent regulation of cAMP/PKA signaling to modulate behavioral responses to stress, we examined the effect of virus-mediated Cdk5 knockout on behaviors induced by acute and chronic stress.

Bilateral stereotactic injection of AAV2-Cre into the ventral striatum caused specific loss of Cdk5 in the area surrounding the injection site of homozygous floxed Cdk5, but not WT, mice (**Fig. 3a–c** and **Supplementary Fig. 7a**). Consistently, PDE4 phosphorylation at the Cdk5 and PKA sites was decreased in ventral striatum of virus-mediated Cdk5 knockout mice (AAV-Cdk5-KO; **Fig. 3b,c**). Consistent with the findings in Cdk5 cKO, AAV-Cdk5-KO mice exhibited reduced immobility in the FST (**Fig. 3d**), increased struggle in TST (**Fig. 3e**) and resistance to chronic stress in the SD procedure (**Fig. 3f**). In addition, AAV-Cdk5-KO showed an increased preference for sucrose in SPT compared with controls (**Fig. 3g**) and resistance to the effect of CUS on sucrose preference (**Fig. 3h**). Further behavioral analysis revealed that virus-mediated Cdk5 knockout in ventral striatum did not affect locomotion, anxiety-like behavior or social interaction (**Supplementary Fig. 7b–e**). Together, these results indicate that Cdk5 functions in the ventral striatum to modulate stress-induced behavioral responses.

In the limbic circuitry, G_s-coupled D1 dopamine receptors of the ventral striatum mediate reward perception via activation of cAMP/PKA signaling, which may be affected in MDD²⁵. To further assess



whether D1 dopamine receptor positive neurons specifically employ Cdk5-dependent regulation of cAMP/PKA signaling to modulate stress-induced behavior, we generated D1 dopamine receptor-specific Cdk5 KO (D1R-Cdk5-KO) mice. Approximately 50% of medium spiny neurons in ventral striatum manifested Cre expression, as reflected by GFP staining as a marker for viral infection of striatal neurons, and loss of Cdk5 (**Supplementary Fig. 8a**). Consequently, Cdk5 was reduced in D1R-Cdk5-KO striatal lysates (**Supplementary Fig. 8b**) and coincided with decreased PDE4 phosphorylation at the Cdk5 and PKA sites (**Supplementary Fig. 8c,d**). As was observed for brain-wide Cdk5 cKO, D1R-Cdk5-KO mice showed markedly reduced immobility in the FST, increased struggle in TST and resistance to chronic SD (**Supplementary Fig. 9a–c**). D1R-Cdk5-KO mice exhibited normal social interaction and increased open arm time in the elevated plus maze (**Supplementary Fig. 9e,f**). Notably, locomotor activity in the D1R-Cdk5-KO mice was normal in social interaction testing and in the elevated plus maze (**Supplementary Fig. 9d,g**), but was increased in cage activity and the open field assay (**Supplementary Fig. 9h,i**). Moreover no difference was observed in the SPT between genotypes (**Supplementary Fig. 10a**). It should be noted that the hyperactivity of the D1R-Cdk5-KO mice, observed only in habituated environments, could have imparted some bias on FST and TST results. Similarly, D1R-Cdk5-KO mice consumed more liquid during daytime (**Supplementary Fig. 10b–d**), possibly obfuscating a clear phenotype in sucrose preference. Accepting these caveats, the Cdk5 cKO, virus-mediated Cdk5 KO in ventral striatum and D1R-Cdk5-KO mice all showed consistent biochemical and behavioral effects supporting an integral role for Cdk5 in stress-induced behavior.

To test the notion that the regulation of cAMP/PKA signaling by Cdk5 in neurons of the ventral striatum is important for stress-induced behavior, we evaluated the effect of PKA inhibition on the

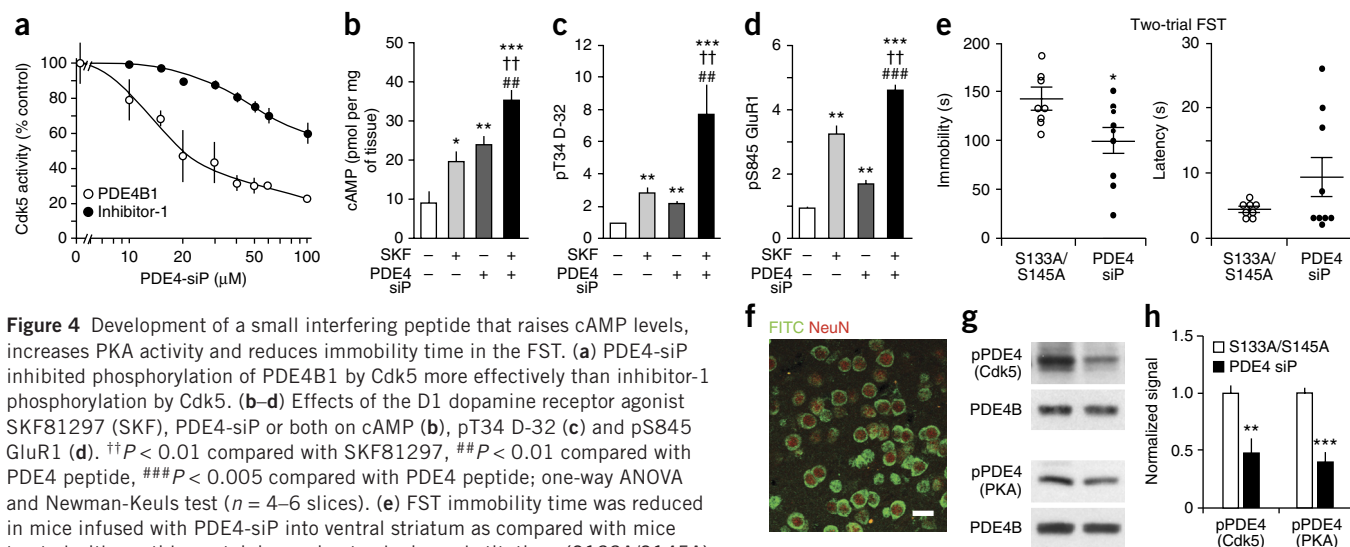


Figure 4 Development of a small interfering peptide that raises cAMP levels, increases PKA activity and reduces immobility time in the FST. **(a)** PDE4-siP inhibited phosphorylation of PDE4B1 by Cdk5 more effectively than inhibitor-1 phosphorylation by Cdk5. **(b–d)** Effects of the D1 dopamine receptor agonist SKF81297 (SKF), PDE4-siP or both on cAMP **(b)**, pT34 D-32 **(c)** and pS845 GluR1 **(d)**. $\dagger\dagger P < 0.01$ compared with SKF81297, $\#\#\# P < 0.001$ compared with PDE4 peptide; one-way ANOVA and Newman-Keuls test ($n = 4–6$ slices). **(e)** FST immobility time was reduced in mice infused with PDE4-siP into ventral striatum as compared with mice treated with peptide containing serine to alanine substitutions (S133A/S145A) (S133A/S145A, $n = 8$; PDE4-siP, $n = 9$; immobility, $P = 0.0285$; latency, $P = 0.1498$). **(f)** Immunostaining of FITC-tagged peptide infused into the ventral striatum. Scale bar represents 25 μm . **(g,h)** PDE4 phosphorylation at the Cdk5 and PKA sites was reduced in mice with intra-striatal infusion of PDE4-siP (S133A/S145A, $n = 5$; PDE4-siP, $n = 6$; pPDE4 (Cdk5), $P = 0.0071$; pPDE4 (PKA), $P = 0.0002$). Whole immunoblot images are included in **Supplementary Figure 13**. All data shown are means \pm s.e.m. $*P < 0.05$, $**P < 0.01$, $***P < 0.001$.

FST phenotype in the D1R-Cdk5-KO and Cdk5 cKO mice. Acute bilateral stereotactic infusion of the specific PKA inhibitor Rp-cAMPS into the ventral striatum of D1R-Cdk5-KO mice increased immobility in the FST to levels comparable to those of WT mice (**Supplementary Fig. 11a**). Likewise, infusion of Rp-cAMPS into the ventral striatum of Cdk5 cKO mice increased FST immobility to levels comparable to those of WT mice (**Supplementary Fig. 11b**). Taken together, these results suggest that disrupting Cdk5-dependent regulation of cAMP/PKA signaling selectively in D1 receptor-positive medium spiny neurons of the ventral striatum alters stress-induced behavioral responses.

Targeting Cdk5/PKA-dependent PDE4 regulation alters stress-induced behaviors

Given that loss of Cdk5 in ventral striatum altered stress-induced behavior, we evaluated more specifically the contribution of the Cdk5/PDE4 regulatory mechanism to these behavioral changes. We developed a 32-amino acid small interfering peptide (PDE4-siP) comprised of the PDE4 sequence encompassing the Cdk5 site together with a membrane-permeabilizing N-terminal penetratin tag. PDE4-siP inhibited Cdk5-dependent phosphorylation of PDE4 *in vitro* with an IC_{50} of 13 μM (**Fig. 4a**). PDE4-siP was selective, as it was less effective at blocking Cdk5-dependent protein phosphatase inhibitor-1 phosphorylation (**Fig. 4a**). Treatment of striatal slices with PDE4-siP elevated cAMP to comparable levels as treatment with SKF81297 (**Fig. 4b**). Simultaneous administration of PDE4-siP and SKF81297 evoked an additive response. The elevation in cAMP levels induced by PDE4-siP treatment was consistently reflected by increases in PKA activity (**Fig. 4c,d**), whereas Cdk5-dependent phosphorylation of DARPP-32 (Thr75) was not decreased (**Supplementary Fig. 12a**).

Given the efficacy of the PDE4-siP *in vitro* and *ex vivo*, we next assessed its effect on FST performance. Acute bilateral stereotactic infusion of PDE4-siP into ventral striatum significantly reduced immobility in the FST ($P = 0.0285$) compared with infusions with control peptides harboring serine-to-alanine substitutions at the Cdk5 and PKA phosphorylation sites (**Fig. 4e**). PDE4-siP infusion had no effect on locomotor activity (**Supplementary Fig. 12b**). Correct placement

of infusion into the ventral striatum and neuronal uptake of the peptide was confirmed histologically using fluorochrome-labeled peptide (**Fig. 4f**). An analogous effect on FST performance was obtained by infusing a poly-arginine-tagged PDE4 peptide, excluding any effects resulting from the penetratin sequence (**Supplementary Fig. 12c**). Mice infused with peptides in which either the PKA or the Cdk5 phosphorylation site were mutated to alanine exhibited normal immobility in FST (**Supplementary Fig. 12d**), underlining the specificity of the PDE4-siP. Consistent with our previous results, infusion of the PDE4-siP significantly reduced PDE4 phosphorylation at the Cdk5 ($P = 0.0071$) and PKA ($P = 0.0002$) sites in the ventral striatum *in vivo* (**Fig. 4g,h**). In contrast, PDE4 phosphorylation levels were unchanged in dorsal striatum, where no PDE4-siP was infused (**Supplementary Fig. 12e**). Together, these data further support the notion that Cdk5/PKA-dependent PDE4 regulation in the ventral striatum contributes substantially to behavioral responses to stress.

DISCUSSION

Using biochemical, pharmacologic and transgenic techniques, we uncovered a molecular mechanism that regulates cAMP signaling via the control of PDE4 by Cdk5 and PKA. In the basal state, Cdk5 primes PDE4 for activation by PKA, thereby providing negative feedback on cAMP signaling. Disruption of the Cdk5-dependent PDE4 priming results in elevated cAMP level and PKA activity, thereby affecting behavioral responses induced by acute and chronic stress.

Moreover, we identified the ventral striatum as a brain region in which this mechanism critically affects behavioral responses to stress. We employed the most commonly used procedures of acute stress, together with measures of anxiety, anhedonia and chronic stress²³. These procedures have been used extensively to measure the effectiveness of antidepressants, although there exists substantial criticism of their interpretation, and the procedures are generally faulted for not effectively modeling depression. The diagnosis of MDD is based on a cluster of highly variable symptoms, including feelings of worthlessness or guilt, fatigue, insomnia, suicidal thoughts and anhedonia. Based on the observation that stress and emotional losses are potential risk factors for MDD, it is believed that understanding

the biological mechanisms underlying behavioral vulnerability and resilience to stress could shed some light on a subset of MDD symptoms. As such, stress-induced behaviors are not reflective of human MDD *per se*, but represent, at best, aspects associated with the human disorder.

Although Cdk5 expression has been suggested to mediate stress responses¹⁴ and contribute to epigenetic programming²⁶, it has not been linked genetically to MDD or other mental illnesses, likely as a result of its essential role in many neuronal and developmental functions. Genome-wide association studies (GWAS) of MDD are in early phases and do not appear to have yet positively identified or confirmed risk factors for depression. Nevertheless, more powerful GWAS and related investigations of MDD are now beginning to emerge^{27,28} and may provide insight needed for the development of animal models that harbor human risk genes, thereby leading to a better understanding of the etiology and pathophysiology of human depression.

Consistent with our findings, the cAMP signaling cascade that mediates monoamine responses has been associated with the neurobiology of mental illnesses, including MDD^{29,30}. Neuroimaging and post-mortem studies have revealed impaired cAMP signaling in MDD patients, and chronic, but not acute, antidepressant treatment upregulates the cAMP system^{29,31,32}. Globally elevated intracellular cAMP levels induce antidepressant effects^{29,32}. Mice deficient in cAMP-specific PDE4 family members show altered behavioral responses to stress^{33,34}. Accordingly, inhibitors of PDE4, notably ones such as rolipram (4-[3-(cyclohexoxy)-4-methoxyphenyl]-2-pyrrolidone), elevate cAMP, affect behavioral responses to stressors in animals and have antidepressant activity in humans^{35–37}. However, adverse side effects, namely intolerable nausea and emesis, have compromised their clinical application in general³⁸. Such effects could possibly be avoided by 'allosteric' PDE4-specific inhibitors that are currently being developed³⁹. In accordance with our hypothesis and results, an alternative strategy is the identification of upstream or downstream regulators of PDE4 that could provide attractive targets for the development of new therapeutics, including antidepressants.

The neural circuitry of depression most likely encompasses several brain regions, including the prefrontal cortex, hippocampus and multiple components of the limbic system^{40,41}. Layer 5 corticostriatal pyramidal cells have been implicated in mediating antidepressant responses via mechanisms involving p11 (ref. 42). Also consistent with our findings, recent studies have implicated cholinergic⁴³, as well as dopaminergic, inputs into NAc medium spiny neurons with depressive symptoms^{19,20,24}. All of these brain regions are modulated by monoaminergic projections from midbrain and brainstem nuclei, providing a rationale for the efficacy of monoaminergic antidepressants.

We found that it was possible to alter behavioral responses to stress through activation of cAMP signaling in the ventral striatum. Cdk5-dependent regulation of cAMP/PKA signaling is consistent with numerous studies showing that Cdk5 contributes to the homeostatic baseline in striatum and that pharmacological or genetic block of Cdk5 activity increases cAMP/PKA signaling or behaviors mediated by Gs-coupled receptors^{5,44,45}. However, Cdk5 inhibition can deplete neurotransmitter release capacity^{46,47}. Indeed, a recent report showed that selective knockout of Cdk5 in midbrain dopamine neurons reduced striatal dopamine levels¹⁶. Paradoxically, this effect was accompanied by a reduction in intracellular cAMP. These effects correlated with reduced motor activity in response to acute stress, prolonged novel environment-related feeding delay, and attenuated sucrose preference. It may be noted that PDE4 expression is relatively low in midbrain dopamine neurons compared with dopaminergic neurons of the striatum⁴⁸. We observed that Cdk5 cKO throughout

the brain, only in the ventral striatum or in D1 dopamine receptor neurons increased struggle in the FST and TST, attenuated social defeat, or enhanced sucrose preference. Nonetheless, it is possible that competing effects may occur in different components of brain circuitry through yet to be determined mechanisms.

Moreover, we found that stress-induced behavioral responses can be affected by targeting cAMP metabolism in D1 dopamine receptor-expressing neurons of the ventral striatum. In particular, our results identify the regulation of PDE4 by Cdk5 as a potential target for the development of new treatments for MDD. Likewise, glutamatergic signaling may provide additional alternative targets for MDD therapy⁴⁹. Drugs that act either on glutamatergic or metabotropic neurotransmission may exert their therapeutic effects via shared mechanisms that integrate calcium and cAMP signaling. To improve on current MDD treatments, it will be imperative to look beyond existing monoamine, neurotrophic and neuroendocrine hypotheses. The development of new antidepressant therapies will undoubtedly benefit from the identification of new molecular players as well as mechanisms shared across current hypotheses. The integration of knowledge from such newly identified molecular targets and advances in clinical research, including viral-mediated gene therapy and deep brain stimulation, are likely to further our understanding of MDD pathophysiology and lead to the development of more effective treatments.

METHODS

Methods and any associated references are available in the [online version of the paper](#).

Note: Any Supplementary Information and Source Data files are available in the online version of the paper.

ACKNOWLEDGMENTS

We thank N. Heintz (Rockefeller University) and GenSat for D1R-Cre mice, K. Deisseroth (Stanford University) for the Dio-Cre vector, C. Burger (University of Wisconsin-Madison) for AAV vectors, H. Ball and Y. Li (University of Texas Southwestern (UTSW) Protein Technology Center) for peptides, the UTSW Animal Resource Center for help with phosphorylation state-specific antibody generation, D.M. Dietz, M. Lutter, M. Kouser and J. Kumar for help with the social defeat procedure, and T. Singh and G. Mettlach for technical assistance. We thank M. Trivedi and the UTSW Depression Center for support. This work was supported by a Brain and Behavior Research Foundation NARSAD Young Investigator Award (K.H.), a pre-doctoral National Research Service Award from the National Institute on Drug Abuse (D.R.B.), a grant from the Darrell K Royal Research Fund for Alzheimer's Research (F.P.) and the California Metabolic Research Foundation (M.D.H.), as well as by US National Institutes of Health grants to A.C.N. and P.G. (MH090963, DA10044), E.J.N. (MH51399), R.T. (GM084249) and J.A.B. (MH79710, MH083711, DA016672, DA018343, DA033485, NS073855).

AUTHOR CONTRIBUTIONS

F.P., K.H., D.R.B., A.H., T.C.T., C.T., J.D., M.W.F., E.Y.Y., M.S.G. and A.N. collected data and analyzed the experiments. F.P., Z.Y., A.C.N., E.J.N., A.N., P.G., R.T., M.D.H. and J.A.B. contributed to study design, supervision and interpretation of the experiments. F.P. and J.A.B. wrote the manuscript.

COMPETING FINANCIAL INTERESTS

The authors declare no competing financial interests.

Reprints and permissions information is available online at <http://www.nature.com/reprints/index.html>.

- Conti, M. & Beavo, J. Biochemistry and physiology of cyclic nucleotide phosphodiesterases: essential components in cyclic nucleotide signaling. *Annu. Rev. Biochem.* **76**, 481–511 (2007).
- Houslay, M.D. Underpinning compartmentalized cAMP signaling through targeted cAMP breakdown. *Trends Biochem. Sci.* **35**, 91–100 (2010).
- Sette, C. & Conti, M. Phosphorylation and activation of a cAMP-specific phosphodiesterase by the cAMP-dependent protein kinase. Involvement of serine 54 in the enzyme activation. *J. Biol. Chem.* **271**, 16526–16534 (1996).

4. MacKenzie, S.J. *et al.* Long PDE4 cAMP-specific phosphodiesterases are activated by protein kinase A-mediated phosphorylation of a single serine residue in upstream conserved region 1 (UCR1). *Br. J. Pharmacol.* **136**, 421–433 (2002).
5. Bibb, J.A. *et al.* Phosphorylation of DARPP-32 by Cdk5 modulates dopamine signalling in neurons. *Nature* **402**, 669–671 (1999).
6. Dhavan, R. & Tsai, L.H. A decade of CDK5. *Nat. Rev. Mol. Cell Biol.* **2**, 749–759 (2001).
7. Angelo, M., Plattner, F. & Giese, K.P. Cyclin-dependent kinase 5 in synaptic plasticity, learning and memory. *J. Neurochem.* **99**, 353–370 (2006).
8. Plattner, F. *et al.* Memory enhancement by targeting Cdk5 regulation of NR2B. *Neuron* **81**, 1070–1083 (2014).
9. Meyer, D.A. *et al.* Ischemic stroke injury is mediated by aberrant Cdk5. *J. Neurosci.* **34**, 8259–8267 (2014).
10. Barnett, D.G. & Bibb, J.A. The role of Cdk5 in cognition and neuropsychiatric and neurological pathology. *Brain Res. Bull.* **85**, 9–13 (2011).
11. Su, S.C. & Tsai, L.H. Cyclin-dependent kinases in brain development and disease. *Annu. Rev. Cell Dev. Biol.* **27**, 465–491 (2011).
12. Fischer, A., Sananbenesi, F., Schrick, C., Spiess, J. & Radulovic, J. Cyclin-dependent kinase 5 is required for associative learning. *J. Neurosci.* **22**, 3700–3707 (2002).
13. Bignante, E.A. *et al.* Involvement of septal Cdk5 in the emergence of excessive anxiety induced by stress. *Eur. Neuropsychopharmacol.* **18**, 578–588 (2008).
14. Bignante, E.A., Paglini, G. & Molina, V.A. Previous stress exposure enhances both anxiety-like behavior and p35 levels in the basolateral amygdala complex: modulation by midazolam. *Eur. Neuropsychopharmacol.* **20**, 388–397 (2010).
15. Zhu, W.L. *et al.* Increased Cdk5/p35 activity in the dentate gyrus mediates depressive-like behavior in rats. *Int. J. Neuropsychopharmacol.* **15**, 795–809 (2012).
16. Zhong, P. *et al.* Cyclin-dependent kinase 5 in the ventral tegmental area regulates depression-related behaviors. *J. Neurosci.* **34**, 6352–6366 (2014).
17. Carlson, J.N., Fitzgerald, L.W., Keller, R.W. Jr. & Glick, S.D. Side and region dependent changes in dopamine activation with various durations of restraint stress. *Brain Res.* **550**, 313–318 (1991).
18. Chrapusta, S.J., Wyatt, R.J. & Masserano, J.M. Effects of single and repeated footshock on dopamine release and metabolism in the brains of Fischer rats. *J. Neurochem.* **68**, 2024–2031 (1997).
19. Tye, K.M. *et al.* Dopamine neurons modulate neural encoding and expression of depression-related behavior. *Nature* **493**, 537–541 (2013).
20. Chaudhury, D. *et al.* Rapid regulation of depression-related behaviors by control of midbrain dopamine neurons. *Nature* **493**, 532–536 (2013).
21. Hawasli, A.H. *et al.* Cyclin-dependent kinase 5 governs learning and synaptic plasticity via control of NMDAR degradation. *Nat. Neurosci.* **10**, 880–886 (2007).
22. Weber, P., Metzger, D. & Chambon, P. Temporally controlled targeted somatic mutagenesis in the mouse brain. *Eur. J. Neurosci.* **14**, 1777–1783 (2001).
23. Nestler, E.J. & Hyman, S.E. Animal models of neuropsychiatric disorders. *Nat. Neurosci.* **13**, 1161–1169 (2010).
24. Schlaepfer, T.E. *et al.* Deep brain stimulation to reward circuitry alleviates anhedonia in refractory major depression. *Neuropsychopharmacology* **33**, 368–377 (2008).
25. Nestler, E.J. & Carlezon, W.A. Jr. The mesolimbic dopamine reward circuit in depression. *Biol. Psychiatry* **59**, 1151–1159 (2006).
26. Mungenast, A.E. & Tsai, L.H. Cognitive function in health and disease: the role of epigenetic mechanisms. *Neurodegener. Dis.* **10**, 191–194 (2012).
27. Song, G.G., Kim, J.H. & Lee, Y.H. Genome-wide pathway analysis in major depressive disorder. *J. Mol. Neurosci.* **51**, 428–436 (2013).
28. Hek, K. *et al.* A genome-wide association study of depressive symptoms. *Biol. Psychiatry* **73**, 667–678 (2013).
29. Dwivedi, Y. & Pandey, G.N. Adenylyl cyclase-cyclicAMP signaling in mood disorders: role of the crucial phosphorylating enzyme protein kinase A. *Neuropsychiatr. Dis. Treat.* **4**, 161–176 (2008).
30. Duman, R.S. & Voleti, B. Signaling pathways underlying the pathophysiology and treatment of depression: novel mechanisms for rapid-acting agents. *Trends Neurosci.* **35**, 47–56 (2012).
31. Fujita, M. *et al.* Downregulation of brain phosphodiesterase type IV measured with (11)C-(R)-rolipram positron emission tomography in major depressive disorder. *Biol. Psychiatry* **72**, 548–554 (2012).
32. O'Donnell, J.M. & Xu, Y. Evidence for global reduction in brain cyclic adenosine monophosphate signaling in depression. *Biol. Psychiatry* **72**, 524–525 (2012).
33. Halene, T.B. & Siegel, S.J. PDE inhibitors in psychiatry—future options for dementia, depression and schizophrenia? *Drug Discov. Today* **12**, 870–878 (2007).
34. Kleppisch, T. Phosphodiesterases in the central nervous system. *Handb. Exp. Pharmacol.* **191**, 71–92 (2009).
35. Zeller, E., Stief, H.J. & Pflug, B. Sastre-y-Hernandez, M. Results of a phase II study of the antidepressant effect of rolipram. *Pharmacopsychiatry* **17**, 188–190 (1984).
36. Zhang, H.T. *et al.* Antidepressant-like profile and reduced sensitivity to rolipram in mice deficient in the PDE4D phosphodiesterase enzyme. *Neuropsychopharmacology* **27**, 587–595 (2002).
37. O'Donnell, J.M. & Zhang, H.T. Antidepressant effects of inhibitors of cAMP phosphodiesterase (PDE4). *Trends Pharmacol. Sci.* **25**, 158–163 (2004).
38. Houslay, M.D., Schafer, P. & Zhang, K.Y. Keynote review: phosphodiesterase-4 as a therapeutic target. *Drug Discov. Today* **10**, 1503–1519 (2005).
39. Burgin, A.B. *et al.* Design of phosphodiesterase 4D (PDE4D) allosteric modulators for enhancing cognition with improved safety. *Nat. Biotechnol.* **28**, 63–70 (2010).
40. Nestler, E.J. *et al.* Neurobiology of depression. *Neuron* **34**, 13–25 (2002).
41. Mayberg, H.S. *et al.* Reciprocal limbic-cortical function and negative mood: converging PET findings in depression and normal sadness. *Am. J. Psychiatry* **156**, 675–682 (1999).
42. Schmidt, E.F. *et al.* Identification of the cortical neurons that mediate antidepressant responses. *Cell* **149**, 1152–1163 (2012).
43. Warner-Schmidt, J.L. *et al.* Cholinergic interneurons in the nucleus accumbens regulate depression-like behavior. *Proc. Natl. Acad. Sci. USA* **109**, 11360–11365 (2012).
44. Bibb, J.A. *et al.* Effects of chronic exposure to cocaine are regulated by the neuronal protein Cdk5. *Nature* **410**, 376–380 (2001).
45. Benavides, D.R. *et al.* Cdk5 modulates cocaine reward, motivation, and striatal neuron excitability. *J. Neurosci.* **27**, 12967–12976 (2007).
46. Kim, S.H. & Ryan, T.A. CDK5 serves as a major control point in neurotransmitter release. *Neuron* **67**, 797–809 (2010).
47. Tan, T.C. *et al.* Cdk5 is essential for synaptic vesicle endocytosis. *Nat. Cell Biol.* **5**, 701–710 (2003).
48. Johansson, E.M., Reyes-Irisarri, E. & Mengod, G. Comparison of cAMP-specific phosphodiesterase mRNAs distribution in mouse and rat brain. *Neurosci. Lett.* **525**, 1–6 (2012).
49. Mathews, D.C., Henter, I.D. & Zarate, C.A. Targeting the glutamatergic system to treat major depressive disorder: rationale and progress to date. *Drugs* **72**, 1313–1333 (2012).

ONLINE METHODS

Antibodies and reagents. Primary antibodies used for immunoblotting and/or immunochemistry are listed in **Supplementary Table 2**. Horseradish peroxidase-conjugated secondary anti-mouse (#31432), anti-rabbit (#31460) and anti-goat (#31402) IgG antibodies were from Thermo Fisher Scientific, Cy3-conjugated anti-rabbit IgG secondary antibody was from Jackson ImmunoResearch Laboratories (711-165-152), and Alexa647-conjugated anti-mouse IgG secondary antibody was from Invitrogen Molecular Probes (Life Technologies; A-21202). AAV2-Cre was from SigmaGen Laboratories. All chemicals and reagents were obtained from Sigma unless stated otherwise. The Cdk5 inhibitor indolinone A was kindly provided by Boehringer Ingelheim. All peptides were synthesized by the UTSW Protein Chemistry Technology Center using the Perseptive Biosystems Pioneer and Applied Biosystems 433 synthesizers. Peptides were verified by mass spectrometry analysis and reversed-phase high-performance liquid chromatography (HPLC). The sequence of the penetratin-tagged PDE4 small interfering peptide (PDE4-siP) was RQIKIWFQNRRMKWKK-ESFLYRSDSDYDLSPKAM; the scrambled-peptide, RQIKIWFQNRRMKWKK-SFDLMSYDEPKSYALDRS; the poly-arginine-tagged PDE4 peptide, RRRRRR-ESFLYRSDSDYDLSPKAM; the S133A peptide, RQIKIWFQNRRMKWKK-EAFLYRSDSDYDLSPKAM; the S145A peptide, RQIKIWFQNRRMKWKK-ESFLYRSDSDYDLAPKAM; the S133A/S145A peptide, RQIKIWFQNRRMKWKK-EAFLYRSDSDYDLAPKAM. The FITC-tag was attached at the C terminus of the siP.

Animals. Animals were maintained on a 12-h light/dark cycle (lights on from 6:00 a.m. to 6:00 p.m.), with access to food and water *ad libitum*. Mice in the C57/BL6 background were obtained from the in-house breeding facility and were housed 2–4 per cage. Cdk5 cKO mice were generated and maintained as previously described²¹. In brief, floxed Cdk5 and Cre-ERT mice were crossed and male offspring at 8 weeks of age were injected with 4-hydroxytamoxifen for 15 d (67 mg per kg of body weight, intraperitoneal). All experiments were performed 2–4 weeks after injections, when the males were 12–14 weeks old. The D1 dopamine receptor-specific Cdk5 KO mouse line (D1R-Cdk5-KO) was generated by crossing homozygous floxed Cdk5 mice with animals bearing a D1 dopamine receptor promoter-driven Cre transgene derived from the founder line EY262 from Gensat (http://www.mmrrc.org/catalog/sds.php?mmrrc_id=17264). Cre expression was evaluated using an adeno-associated virus (AAV5) harboring the Dio-YFP Cre reporter (kindly provided by K. Deisseroth). All experimental procedures were reviewed and approved by the University of Texas Southwestern Institutional Animal Care and Use Committee and conducted in accordance with the US National Institutes of Health *Guide for the Care and Use of Laboratory Animals*.

Behavioral analysis. The Porsolt FST was conducted as described previously⁵⁰. In brief, 10–12-week-old mice were placed into a vertical glass cylinder filled with water (25 °C). In the one-trial FST version, the mice spent 8 min in the water. In the two-trial FST, the mice were placed for 10 min in the cylinder and 24 h later re-exposed for 8 min. For all trials, immobility was scored for the interval between 2 and 6 min by two independent researchers. The TST was conducted as described previously⁵⁰. SD and social interaction testing were performed as described previously⁵¹. For the sucrose preference test, mice were individually housed in cages with two bottles. On days 1 and 2, both bottles contained water, on days 3 and 4 they were filled with water containing 1% sucrose (wt/vol), on days 5 to 9 one bottle was filled with water the other with 1% sucrose solution. The total volume of liquid consumed for each bottle was monitored on each day. The location of the bottles was inverted every day to avoid location bias. Sucrose preference was calculated as the fraction of sucrose solution consumed divided by the total amount of liquid consumed. Horizontal spontaneous locomotor activity was monitored in clean home cages with minimal bedding for 1 h in the dark. Mice were individually placed in standard polypropylene cages (15 × 25 cm) located in chambers equipped with a computer-monitored infrared photobeam system (Photobeam Analysis Software, San Diego Instruments). Locomotor activity was measured as sequential adjacent beam breaks and indicated as locomotor counts. The open field assay was performed in 40 × 40-cm opaque polypropylene boxes and locomotion was traced with a video tracking system (Noldus EthoVision). After at least 1 h of habitation, mice were transferred into the open field box and left to explore for 20 min in dim light condition. In between trials, the boxes

were thoroughly cleaned with Process NPT (Steris). The elevated plus maze was conducted using a black, plexiglass elevated plus maze (plus-shaped apparatus with two open and two enclosed arms, each arm 33 cm long and 5 cm wide with 25 cm high walls on closed arms, elevated 80 cm from the floor). After at least 1 h of habitation, mice were placed in the center of the elevated plus maze and left to explore for 5 min in dim light condition. Locomotion was traced with a video tracking system (Noldus EthoVision) and used to analyze time spent in the open and closed arms, time spent in the center and total locomotor activity. In between trials, the maze was thoroughly cleaned with Process NPT (Steris).

The CUS procedure was performed as adapted from ref. 52. In brief, single-housed mice are exposed to two stressors in 24 h for 14 d. The stressors include exposure to new and/or adverse environment for 2–4 h (that is, plastic cage without bedding, cage grid, tilted cage, cage filled with thin layer of water, cage with damp saw dust, cage containing bedding with rat odor), overnight food and water deprivation, change of light cycle (reverse light cycle, split light cycle in 3 h blocks for 12 h), swimming for 5 min, exposure to aggressor for 5 min, restraint stress for 45 min, tail suspension for 6 min. After 14 d of CUS, the mice were assessed for sucrose preference as described above.

All behavioral experiments were carried out with the experimenter blind to genotype and /or treatment history.

Stereotaxic infusion. Mice were anesthetized with isoflurane, placed in a stereotaxic frame (Kopf Instruments) and microsyringes (Hamilton) were inserted to bilaterally target the NAc (anterior-posterior to bregma +1.50 mm, medial/lateral ±1.4 mm, depth –3.90 mm). The injection volume was 1 µl of PDE4-siP (115 µM), scrambled siP (115 µM) and Rp-cAMPs (45 µM) per cerebral hemisphere. Animals were allowed to recover from surgery for 45 min post-infusion of PKA inhibitor and for 90 min post-infusion of siP before behavioral testing. Behavioral performance in mice 45 min post-anesthesia was not different from mice without anesthesia. Target regions were confirmed by detection of the infusion of a FITC-labeled siP via immunostaining for FITC with NeuN counterstaining. NAc-specific Cdk5 CKO (NAc-CKO) was achieved in adult (8–10 weeks old) male homozygous fCdk5 mice via bilateral stereotaxic delivery of AAV2-Cre (~6.4 × 10⁸ particles, 1 µl per hemisphere) to the NAc (anterior-posterior to bregma +1.50 mm, medial/lateral ±1.4 mm, depth –3.90 mm).

Electrophysiological recordings. Recordings of whole-cell ion channel currents used standard voltage-clamp techniques^{8,53}. The internal solution consisted of the following (in mM): 180 N-methyl-D-glucamine, 40 HEPES, 4 MgCl₂, 0.1 BAPTA, 12 phosphocreatine, 3 Na₂ATP, 0.5 Na₂GTP and 0.1 leupeptin, pH 7.2–7.3, 265–270 mOsm/l. The external solution consisted of the following (in mM): 127 NaCl, 20 CsCl, 10 HEPES, 1 CaCl₂, 5 BaCl₂, 12 glucose, 0.001 tetrodotoxin and 0.02 glycine, pH 7.3–7.4, 300–305 mOsm. Recordings were obtained with an Axon Instruments 200B patch-clamp amplifier that was controlled and monitored with an IBM personal computer running pClamp (version 10) with a DigiData 1440 series interface (Axon Instruments). Electrode resistances were typically 3–5 MΩ in the bath. After seal rupture, the series resistance was between 4–10 MΩ and periodically monitored. The cell membrane potential was held at –70 mV. The application of NMDA (100 µM) evoked a partially desensitizing inward current that could be blocked by the NMDA receptor antagonist D-AP5 (50 µM). NMDA was applied for 2 s every 30 s to minimize desensitization-induced decrease of current amplitude. Drugs were applied with a gravity-fed ‘sewer pipe’ system. The array of application capillaries (~150 µm inner diameter) was positioned a few hundred micrometers from the cell under study. Solution changes were affected by the SF-77B fast-step solution stimulus delivery device (Warner Instruments).

Acute striatal slices, quantitative immunoblotting and histology. Striatal slices were prepared as previously described⁵⁴ and were treated with 25 µM PDE4-siP for 60 min and 1 µM SKF81297 for 10 min unless stated otherwise. Quantitative immunoblotting was conducted using standard methodology⁵. Immunohistochemical analysis was conducted as described previously⁵⁵. Immunoblot signals were normalized to β-actin, GAPDH and/or coomassie blue staining. Immunoblots of phospho-specific antibodies were normalized to signals from corresponding total protein blots. Fluorescent *in situ* hybridization was conducted as described previously^{21,45}. Golgi-Cox staining was performed as described for the FD Rapid GolgiStain Kit (FD NeuroTechnologies).

Quantitation of cAMP, cGMP and catecholamines, PDE activity assays, and BRET analysis. The cAMP assay was performed using cAMP Biotrak Enzyme-ImmunoAssay kit (Amersham) according to manufacturer's instructions. The cGMP assay was conducted using cGMP Direct Biotrak Enzyme-ImmunoAssay kit (Amersham) according to manufacturer's instructions. HPLC with electrochemical detection was performed as described⁵⁶ to quantify levels of DA, and its metabolites 3,4-dihydroxyphenylacetic acid (DOPAC), homovanillic acid (HVA), and 3-methoxytyramine (3-MT), as well as 5-HT from mouse striatum. Neurotransmitter monoamines and metabolites were detected using an ESA CoulArray electrochemical detector with a model 5014B cell set to a potential of +220 mV. PDE activity was assessed in lysates from dissected striatum and Cos-1 cells transfected with PDE4 site-directed mutants by modification of a two-step radioenzymatic assay^{57,58}. BRET analysis was conducted in stably transfected HEK293 cells as described previously⁵⁹. Effects of indolinone A on PKA-dependent phosphorylation was also assessed in these cells.

Protein purification, *in vitro* phosphorylation reactions and immunoprecipitation-kinase assay. Recombinant PDE4B1 fused with maltose binding protein (MBP) was purified as previously described⁶⁰. *In vitro* phosphorylation reactions, quantitative analysis and immunoprecipitation-kinase assays were also conducted as described previously^{5,21}.

Mass spectrometry and generation of phosphorylation state-specific PDE4B antibodies. HPLC/mass spectrometry was carried out using methodologies described⁶¹. Polyclonal phosphorylation state-specific antibodies detecting the PKA and Cdk5 phosphorylation sites on PDE4 were generated and affinity purified using techniques described⁶².

Statistical analysis. All data are expressed as mean \pm s.e.m. Statistical analysis was performed using the Student's *t* test, one-way analysis of variance (ANOVA) and two-way ANOVA with Bonferroni *post hoc* comparison unless stated otherwise. Data distribution was assumed to be normal, but this was not formally tested. Statistical test were performed two-sided unless stated otherwise. No statistical

methods were used to predetermine sample sizes, but our sample sizes are similar to those generally employed in comparable studies.

A **Supplementary Methods Checklist** is available.

50. Castagne, V., Moser, P., Roux, S. & Porsolt, R.D. Rodent models of depression: forced swim and tail suspension behavioral despair tests in rats and mice. *Curr. Protoc. Neurosci.* **8.8**, 10A (2011).
51. Golden, S.A., Covington, H.E. III., Berton, O. & Russo, S.J. A standardized protocol for repeated social defeat stress in mice. *Nat. Protoc.* **6**, 1183–1191 (2011).
52. Willner, P., Towell, A., Sampson, D., Sophokleous, S. & Muscat, R. Reduction of sucrose preference by chronic unpredictable mild stress, and its restoration by a tricyclic antidepressant. *Psychopharmacology (Berl.)* **93**, 358–364 (1987).
53. Yuen, E.Y. *et al.* Repeated stress causes cognitive impairment by suppressing glutamate receptor expression and function in prefrontal cortex. *Neuron* **73**, 962–977 (2012).
54. Nishi, A., Snyder, G.L. & Greengard, P. Bidirectional regulation of DARPP-32 phosphorylation by dopamine. *J. Neurosci.* **17**, 8147–8155 (1997).
55. Nishi, A. *et al.* Distinct roles of PDE4 and PDE10A in the regulation of cAMP/PKA signaling in the striatum. *J. Neurosci.* **28**, 10460–10471 (2008).
56. Frank-Cannon, T.C. *et al.* Parkin deficiency increases vulnerability to inflammation-related nigral degeneration. *J. Neurosci.* **28**, 10825–10834 (2008).
57. Marchmont, R.J. & Houslay, M.D. A peripheral and an intrinsic enzyme constitute the cyclic AMP phosphodiesterase activity of rat liver plasma membranes. *Biochem. J.* **187**, 381–392 (1980).
58. Lobban, M., Shakur, Y., Beattie, J. & Houslay, M.D. Identification of two splice variant forms of type-IVB cyclic AMP phosphodiesterase, DPD (rPDE-IVB1) and PDE-4 (rPDE-IVB2) in brain: selective localization in membrane and cytosolic compartments and differential expression in various brain regions. *Biochem. J.* **304**, 399–406 (1994).
59. Jiang, L.I. *et al.* Use of a cAMP BRET sensor to characterize a novel regulation of cAMP by the sphingosine 1-phosphate/G13 pathway. *J. Biol. Chem.* **282**, 10576–10584 (2007).
60. Murdoch, H. *et al.* Isoform-selective susceptibility of DISC1/phosphodiesterase-4 complexes to dissociation by elevated intracellular cAMP levels. *J. Neurosci.* **27**, 9513–9524 (2007).
61. Zhao, Y., Zhang, W. & White, M.A. Capillary high-performance liquid chromatography/mass spectrometric analysis of proteins from affinity-purified plasma membrane. *Anal. Chem.* **75**, 3751–3757 (2003).
62. Czernik, A.J., Mathers, J. & Mische, S.M. Phosphorylation state-specific antibodies. in *Regulatory Protein Modification: Techniques and Protocols Neuromethods, Vol. 30* (ed. H.C. Hemmings, Jr.) 219–250 (Humana Press, 1997).